Neuroradiology
https://doi.org/10.1007/s00234-022-03013-9

DIAGNOSTIC NEURORADIOLOGY

A Bayesian estimation method for cerebral blood flow measurement by area-detector CT perfusion imaging

Kazuhiro Murayama[1] · Ewoud J. Smit[2] · Mathias Prokop[2] · Yoshihiro Ikeda[3] · Kenji Fujii[3] · Ichiro Nakahara[4] · Satomu Hanamatsu[1] · Kazuhiro Katada[1] · Yoshiharu Ohno[1] · Hiroshi Toyama[1]

Received: 1 April 2022 / Accepted: 6 July 2022

Abstract

Purpose Bayesian estimation with advanced noise reduction (BEANR) in CT perfusion (CTP) could deliver more reliable cerebral blood flow (CBF) measurements than the commonly used reformulated singular value decomposition (rSVD). We compared the efficacy of CBF measurement by CTP using BEANR and rSVD, evaluating both relative to *N*-isopropyl-*p*-[(123) I]- iodoamphetamine (^{123}I-IMP) single-photon emission computed tomography (SPECT) as a reference standard, in patients with cerebrovascular disease.

Methods Thirty-one patients with suspected cerebrovascular disease underwent both CTP on a 320 detector-row CT system and SPECT. We applied rSVD and BEANR in the ischemic and contralateral regions to create CBF maps and calculate CBF ratios from the ischemic side to the healthy contralateral side (CBF index). The analysis involved comparing the CBF index between CTP methods and SPECT using Pearson's correlation and limits of agreement determined with Bland–Altman analyses, before comparing the mean difference in the CBF index between each CTP method and SPECT using the Wilcoxon matched pairs signed-rank test.

Results The CBF indices of BEANR and ^{123}I-IMP SPECT were significantly and positively correlated ($r = 0.55$, $p < 0.0001$), but there was no significant correlation between the rSVD method and SPECT ($r = 0.15$, $p > 0.05$). BEANR produced smaller limits of agreement for CBF than rSVD. The mean difference in the CBF index between BEANR and SPECT differed significantly from that between rSVD and SPECT ($p < 0.001$).

Conclusions BEANR has a better potential utility for CBF measurement in CTP than rSVD compared to SPECT in patients with cerebrovascular disease.

Keywords Bayesian estimation · Singular value decomposition · CT perfusion · ^{123}I-IMP SPECT · Cerebrovascular disease

✉ Kazuhiro Murayama
kmura@fujita-hu.ac.jp

Ewoud J. Smit
Ewoud.Smit@radboudumc.nl

Mathias Prokop
Mathias.Prokop@radboudumc.nl

Yoshihiro Ikeda
Yoshihiro3.ikeda@medical.canon

Kenji Fujii
kenji3.fujii@medical.canon

Ichiro Nakahara
ichiro@mub.biglobe.ne.jp

Satomu Hanamatsu
st000mthanmz7@yahoo.co.jp

Kazuhiro Katada
kkatada@fujita-hu.ac.jp

Yoshiharu Ohno
yohno@fujita-hu.ac.jp

Hiroshi Toyama
htoyama@fujita-hu.ac.jp

[1] Department of Radiology, Fujita Health University School of Medicine, 1-98 Dengakugakubo, Kutsukake-Cho Toyoake, Aichi 470-1101, Japan

[2] Department of Radiology and Nuclear Medicine, Radboud University Medical Center, Geert Grooteplein Zuid 10, 6525 GA Nijmegen, The Netherlands

[3] Canon Medical Systems Corporation, 1385 Shimoishigami, Otawara, Tochigi 325-8550, Japan

[4] Department of Comprehensive Strokology, Fujita Health University School of Medicine, 1-98 Dengakugakubo, Kutsukake-Cho Toyoake, Aichi 470-1101, Japan

Published online: 18 July 2022

Introduction

CT perfusion (CTP) imaging may have several clinical advantages over other modalities when assessing ischemic stroke, such as wider availability, shorter examination time, higher spatial resolution, and the ability to apply simple mathematical models for quantification [1–3]. Nuclear medicine studies with single-photon emission computed tomography (SPECT) of N-isopropyl-p- [(123) I] -iodoamphetamine (123I-IMP) are widely used to image regional brain perfusion clinically and have been put forward as the reference standard when estimating ischemic areas in patients with cerebrovascular disease (CVD) [4]. Area-detector (AD) CTP, a well-established method for assessing cerebral blood flow (CBF), is well correlated with SPECT [5].

Since 2009, contrast-enhanced (CE) AD-CTP has been performed using 320-detector-row CT systems for evaluating entire intracranial circulation in patients with CVD [6]. Furthermore, several randomized controlled trials for endovascular thrombectomy since 2015 have suggested that CTP imaging can help distinguish infarcts from penumbras and determine the clinical indication of endovascular thrombectomy in acute ischemic stroke using time to maximum of the tissue residue function (T_{max}) [7–9]. The most widely used post-processing method for CTP is the singular value decomposition (SVD), which is applied as a delay-sensitive or -insensitive algorithm to perform quick calculations [10]. However, the CTP parameters derived from SVD can be sensitive to noise [11, 12] and inaccurate for visualizing the ischemic area by underestimating the mean transit time (MTT) increases and cerebral CBF decreases [13].

An alternative deconvolution algorithm to SVD has been proposed that applies Bayesian estimation based on a probabilistic approach to generate a probability distribution for the CTP parameters [14, 15]. This method is less sensitive to noise and shows better accuracy and image quality, and as such, may enhance the determination of abnormal perfusion and infarcts [16]. By calculating the delay in CT perfusion independent of the MTT values, it can also give highly accurate estimates of the delay and ischemic core values [17]. Therefore, Bayesian estimation for CTP may offer more reliable CBF measurement than delay-insensitive reformulated SVD (rSVD), in routine clinical practice [18]. However, no studies have directly compared the efficacies of Bayesian estimation and rSVD relative to an ^{123}I-IMP SPECT reference standard between areas of ischemic and normal perfusion.

We hypothesized that CBF values derived by Bayesian estimation with advanced noise reduction (BEANR), compared to rSVD, will accurately estimate the ischemic areas in patients with CVD. We aimed to compare the efficacy of CBF measurement by CTP using the BEANR and rSVD methods relative to ^{123}I-IMP SPECT in patients with CVD.

Materials and methods

Protocol, support, and funding

This retrospective study was approved by the Institutional Review Board of Fujita Health University and was technically and financially supported by Canon Medical Systems Corporation. Two of the authors are employees of Canon Medical Systems (Y. I and K.F), but did not have control over any of the data used in this study. Two board-certified radiologists (K.M. and Y.O. with 12 and 22 years of experience, respectively) visually selected which target ROIs were within the ischemic MCA territory on SPECT.

Subjects

From July 2015 to March 2018, a total of 72 consecutive patients suspected of ischemic cerebrovascular disease, and who underwent contrast-enhanced CTP examinations with 320-detector row CT and SPECT imaging at our institution, were retrospectively included in this study (Fig. 1). The inclusion criteria were the following: (1) cases suspected ischemic cerebrovascular diseases, (2) cases performed both CTP and ^{123}I-IMP SPECT of the brain, and (3) cases with a CBF laterality of more than 10% in the ICA or MCA territories on SPECT imaging. Of these, 41 cases were excluded due to less than 10% CBF laterality ($n=27$), incomplete CTP and SPECT study protocols ($n=8$), ischemia in except for the ICA or MCA territories ($n=4$), and because therapeutic interventions were performed between CTP and SPECT imaging ($n=2$). We performed CTP and ^{123}I-IMP SPECT examinations within a 3-week interval (mean 17 days).

CTP examination

All CTP examinations were performed with a 320-detector-row CT scanner (Aquilion ONE, Canon Medical Systems Corporation, Ōtawara, Tochigi, Japan) using dynamic volumetric scan without helical imaging. First, we performed dynamic volumetric CT of the whole brain within a 16-cm area using the following parameters: 320 × 0.5 mm collimation, 80 kVp, 70 mA for arterial phase, 30 mA for venous phase, 1 s gantry rotation time, matrix 512 × 512 and field of view of 240 mm. All dynamic CT images were reconstructed using a brain kernel (FC41, Canon Medical Systems) with a filtered back projection for 1 mm section thickness reconstruction. In all patients, we used a dual-head power injector (Dual Shot GX; Nemoto Kyorindo, Tokyo, Japan) to administer a bolus of iodinated contrast material (iopamidol 250 mgI/kg body weight; Iopamiron 370, Bayer Healthcare)

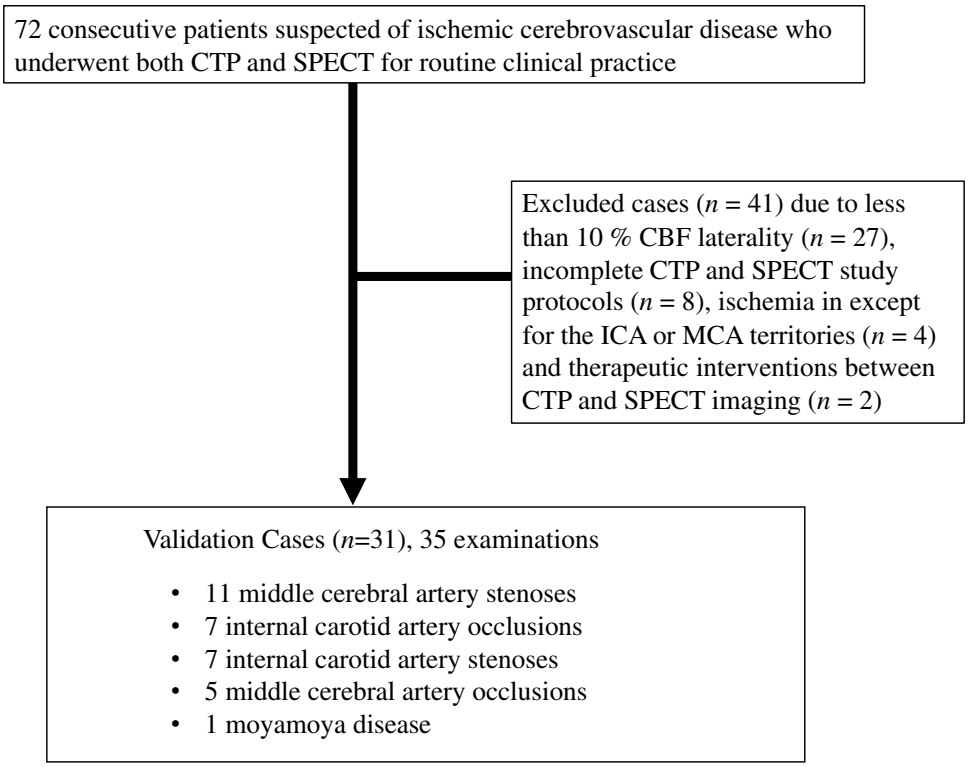

Fig. 1 Flow chart of the study population

through a cubital vein for 10 s, followed by saline solution (30 mL) at the same rate.

Dynamic CT data were first acquired every 2 s in the arterial phase and then every 5 s in the venous phase until the second pass [19]. This produced a series of 21 images at 5, 7, 9, 11, 13, 15, 17, 19, 21, 23, 25, 27, 29, 31, 33, 35, 40, 45, 50, 55, and 60 s from injection. The estimated CT dose index volume ($CTDI_{vol}$) on the CT console was recorded for each patient (61.6 mGy for each dynamic CT study). The estimated dose-length product was calculated as 985.6 mGy·cm ($CTDI_{vol} \times$ scanning length), giving an estimated effective dose of 2.27 mSv in this protocol.

SPECT examination

All SPECT data were collected (continuous mode, 90 s per cycle, 4 cycles, 5 repeats) 15 min after the intravenous injection of 222 MBq (6 mCi) ^{123}I-IMP (patient in quiet room with eyes closed), using a commercially available triple-detector γ-camera with a fan-beam collimator (GCA-9300R, Canon Medical Systems, Ōtawara, Japan). The acquisition parameters were as follows: matrix size, 128 × 128; collection window, 159 keV (± 10%); pixel size, 1.76 mm; scatter correction, triple-energy window method [20]; and acquisition time, 30 min. SPECT data sets were then reconstructed with the following settings: pixel size, 1.72 mm; section thickness, 1.72 mm; and filtered back projection with Ramp and Butterworth filter as pre-smoothing (order, 4; cutoff frequency, 0.58 cycles/cm). We also examined head CT findings using a commercially available CT scanner (Biograph mCT, Siemens Medical Solutions, Erlangen, Germany) for CT-based attenuation correction [21, 22], according to a standardized protocol with the following settings: 120 kV, 410 mAs, automatic exposure control, tube rotation at 1 s per rotation, 32 × 1.2 mm detector collimation, 0.55° beam pitch and 3 mm section thickness. We then reconstructed the CT data to a 0.59-mm pixel size to match the SPECT data, fused the images, and performed CT-based attenuation correction after overlaying the separate SPECT and CT images based on a mutual information method, using commercially available positioning software in the Vitrea workstation (SPECT Viewer, Canon Medical Systems Corporation, Otawara, Tochigi, Japan).

The rSVD with conventional process and the BEANR method for CTP

Figure 2 shows a flow chart of the rSVD with the conventional process. First, we performed a three-dimensional rigid registration to align the anatomical location of all volumes over time. After motion alignment, a Gaussian spatial filter, kernel size 21 × 21 × 21 was applied to the image data. This filter is limiting to surrounding tissue; therefore, the spatial resolution is not preserved. In addition, this filter includes vascular-pixel elimination to avoid blurring vessels [23]. Second, the CTP post-processing using the rSVD method

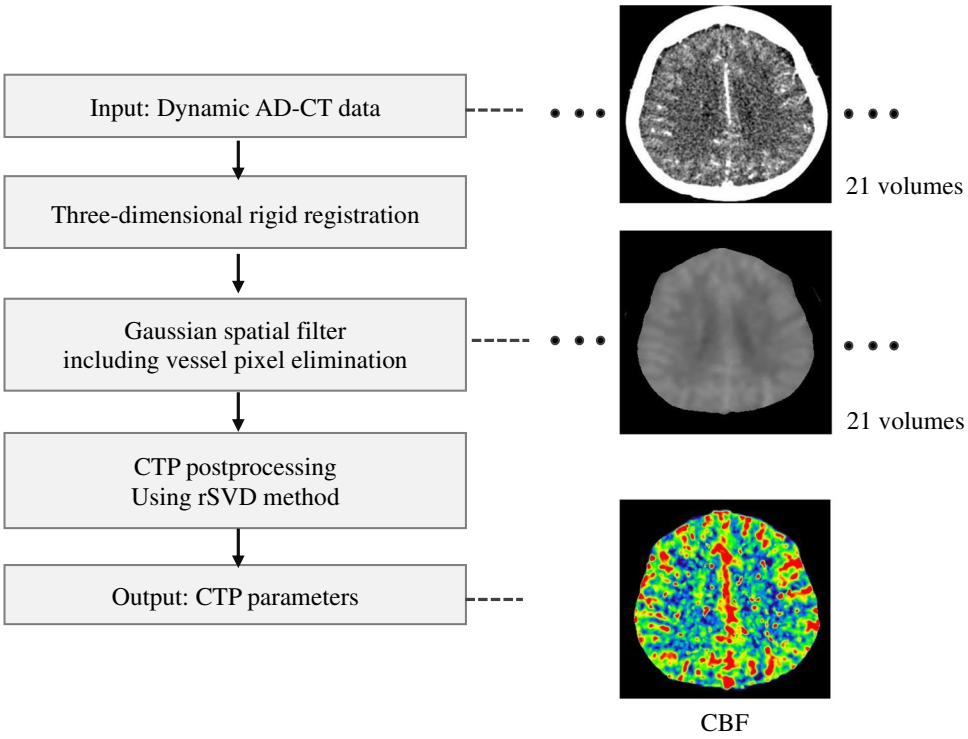

Fig. 2 The rSVD with conventional process. The three-dimensional rigid registration is used to coordinate the anatomical location of all volumes over time. Gaussian spatial filter is applied to reduce noise with vascular-pixel elimination. The parametric CTP maps are generated using the rSVD method

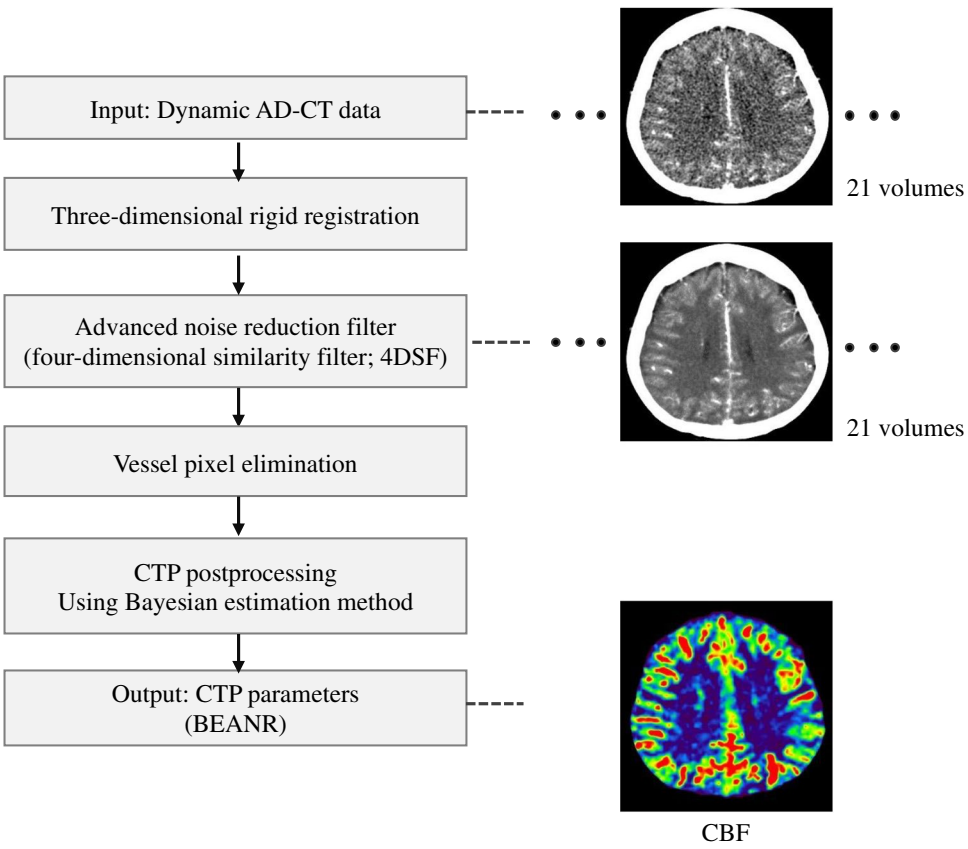

Fig. 3 The Bayesian estimation method with advanced noise reduction. The three-dimensional rigid registration is performed to align the anatomical location of all volumes over time. An advanced noise reduction filter is applied to reduce noise with vascular-pixel elimination. The parametric CTP maps are generated using the Bayesian estimation method

consisted of inputting the filtered image with the Gaussian spatial filter.

Figure 3 shows a flow chart of the BEANR method. First, a three-dimensional rigid registration is applied as the conventional rSVD process. After motion alignment, a newly developed advanced noise reduction filter, the four-dimensional similarity filter (4D-SF), was applied to the image data [24, 25]. This filter used per-voxel similarity within the 4D acquisition sequence to average identically perfused tissues by similar time-density curves. This allowed strong noise reduction without blurring vessels by searching for voxels with similar dynamic behavior globally, without limiting to surrounding tissue, before averaging them by preserving spatial resolution or temporal information [24, 25]. The 4D-SF has a threshold to reject dissimilar voxels in the process of searching for voxels with similar dynamic behavior. Therefore, the 4D-SF can reduce noise without losing the temporal information of time density curves even if the voxels with similar dynamic behavior include distant voxels (e.g., along elongated vessels or skull). In addition, vascular-pixel is eliminated from the filtered image.

Second, the CTP postprocessing by Bayesian estimation consisted of inputting the filtered image with the 4D-SF. We obtained the CTP parameters from the residual function $R(t)$, derived from the deconvolution of the concentration time curves by the arterial input function, which we calculated based on a model-dependent approach for Bayesian estimation according to the following regulation model [15]: (i) $R(t) = 0$ for $t < \tau$, (ii) $R(\tau) = 1$, and (iii) $R(t)$ is smooth for $t \geq \tau$, where τ is the tracer delay. In the SVD method, $R(t)$ is derived using a model-independent approach. Whereas CTP post-processing using the SVD method includes conventional local spatial filtering, the BEANR method does not include a spatial filter because the 4D-SF reduces noise sufficiently. This image filtering process using 4D-SF and CTP postprocessing were commercially supported by Canon Medical Systems Corporation and were performed using commercially available software on a Vitrea workstation (Brain Perfusion 4D, Vital Images, Minnetonka, MN, USA).

Analysis of CTP images

All dynamic CT data were transferred to commercially available software on the Vitrea workstation (Brain Perfusion 4D, Vital Images), and whole brain CBF maps were generated computationally using the rSVD method and the BEANR method in a several minutes after dynamic CT scanning. In each subject, all SPECT data were also transferred to commercially available software on the Vitrea workstation (Mirada XD, Vital Images), aligned to the original CTP data with semi-automatic rigid registration, and resampled to the same slice planes as the original CTP data. Alignment and resampling allowed measurement of CBF values from the same anatomical locations. We selected three target slice levels to investigate the CBF index: basal ganglia, body of the lateral ventricle, and centrum semiovale.

For regional CBF measurements, the 72 circular regions of interest (ROIs; 36-pixel diameters) were automatically placed bilaterally along the cerebral cortex at 5° steps from each image center on ^{123}I-IMP SPECT maps at the three target levels. ROIs were then copied to the same location on CBF maps, using the rSVD and BEANR methods to measure regional CBF values at the same anatomical locations with an in-house MATLAB code (The MathWorks Inc., Natick, MA, USA) (Fig. 4). Two board-certified radiologists ([Blinded] and [Blinded] with 12 and 22 years of experience, respectively) visually selected which target ROIs were within the ischemic MCA territory on SPECT. In each slice, the regional CBFs of the MCA areas were averaged to generate CBF values for rSVD, BEANR, and SPECT. In this study, a CBF ratio from the ischemic side to the healthy

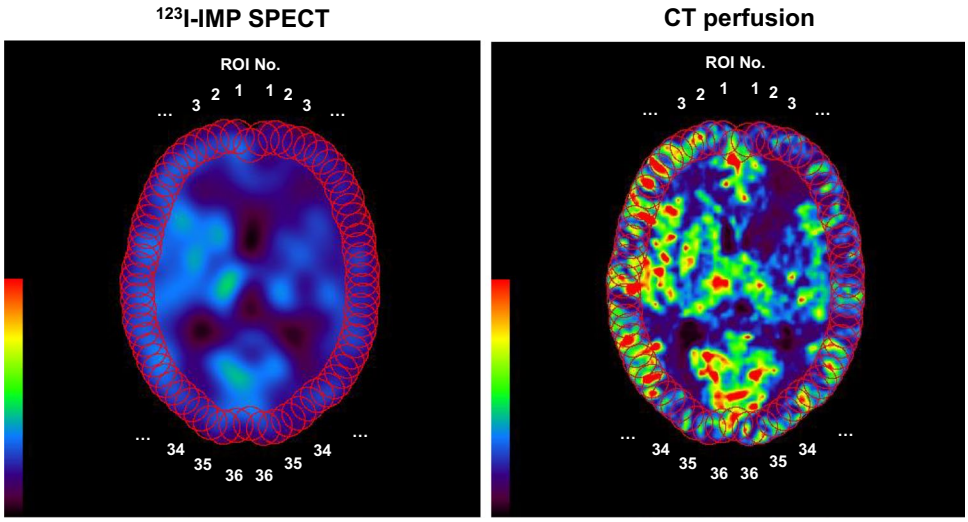

Fig. 4 An example ROI measurement (L to R: ^{123}I-IMP SPECT image, 5-mm CT perfusion-CBF map). ROIs were automatically placed bilaterally along the cerebral cortex every five-step degree from each image center on the ^{123}I-IMP SPECT maps. The ROIs were then copied to the same location on the CBF maps by rSVD and BEANR to measure the regional CBF values at the same anatomical locations

contralateral side was calculated in the MCA area (CBF index) with the following formula:

$$\text{CBFindex} = \frac{\text{regional CBF value in ischemic MCA area}}{\text{regional CBF value in healthy contralateral MCA area}}$$

Statistical analysis

To assess interobserver agreement for the CBF index, we used Person's correlation of individual index measurements for an average of two measurements by each investigator. In addition, interobserver agreement for the CBF index was determined as the limit of agreement determined with the Bland–Altman analysis [26].

To evaluate the difference in quantitative CBF values between the ischemic side and the healthy contralateral side, Wilcoxon matched pair signed rank tests were used to compare the CBF values using ^{123}I-IMP SPECT and each CTP method between the ischemic side and the healthy contralateral side.

To evaluate the relationships between the CBF indices of each CTP and SPECT, the correlations with the CBF indices between each CTP and SPECT images were statistically evaluated by Pearson's correlation. To determine CBF index differences between two CTP techniques, mean differences in CBF index between each CTP method and SPECT imaging were compared by means of Wilcoxon matched pair signed rank tests. Finally, the limits of agreement between any two measures were assessed by Bland–Altman analysis [26].

A p-value less than 0.05 was considered significant in each statistical analysis. All statistical analyzes were performed by JMP 14 (SAS Institute Inc. Japan, Tokyo, Japan) and Graph Pad PRISM (version 7; GraphPad Software, San Diego, CA, USA).

Results

Figures 5 and 6 show representative cases. Eventually, this study group consisted of 31 patients (23 men, 8 women; mean age, 67.1 years; age range, 44 to 78 years) with acute ($n = 20$) and chronic ($n = 11$) ischemic stroke. The diagnoses consisted of 11 MCA stenoses, 7 internal carotid artery (ICA) occlusions, 7 ICA stenoses, 5 MCA occlusions, and 1 moyamoya disease.

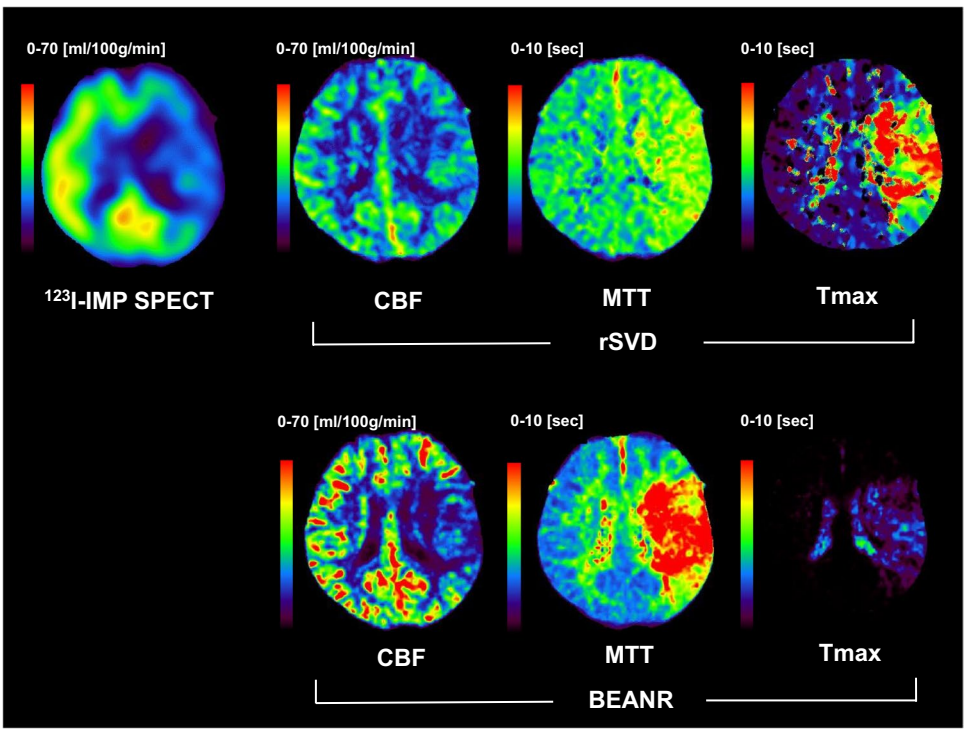

Fig. 5 A 78-year-old female patient with left MCA occlusion (L to R: ^{123}I-IMP SPECT image, CBF, MTT and Tmax of rSVD and BEANR). The ^{123}I-IMP SPECT image shows a low perfusion area in the left cerebrum. BEANR more clearly shows the decreased CBF and prolonged MTT areas in the ischemic region compared to rSVD. Tmax of rSVD is overestimated compared to BEANR. The regional CBF results of rSVD were 27.9 ml/100 g/min in the ischemic region and 35.3 ml/100 g/min in the healthy contralateral side (CBF index: 0.79). The regional results of the CBF of BEANR were 24.8 ml/100 g/min in the ischemic region and 50.5 ml/100 g/min on the healthy contralateral side (CBF index: 0.49). In addition, compared to rSVD, the CBF maps from BEANR better matched those from ^{123}I-IMP SPECT. BEANR also more clearly showed the difference between affected and unaffected sides

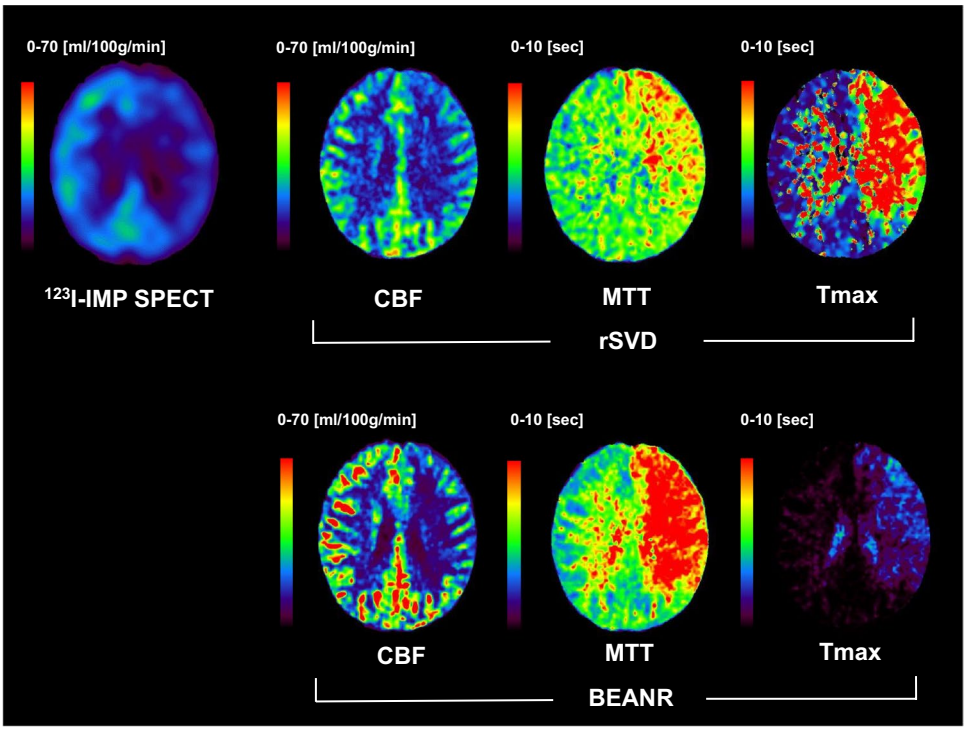

Fig. 6 A 61-year-old male patient with left ICA stenosis (L to R: ^{123}I-IMP SPECT image, CBF, MTT, and Tmax of rSVD and BEANR). The ^{123}I-IMP SPECT image shows a low perfusion area in the left cerebrum. BEANR more clearly shows the decreased CBF and prolonged MTT areas in the ischemic region compared to rSVD. Tmax of rSVD is overestimated compared to BEANR. The results of the regional CBF of rSVD were 29.2 ml/100 g/min in the ischemic region and 33.7 ml/100 g/min in the healthy contralateral side (CBF index: 0.87). The regional results of the CBF of BEANR were 28.3 ml/100 g/min in the ischemic region and 45.7 ml/100 g/min in the healthy contralateral side (CBF index: 0.62). The CBF map of BEANR shows the regional difference in CBF more clearly than ^{123}I-IMP SPECT

As for interobserver agreement on assessments of all the indices, the correlation and the limits of agreement between the two investigators demonstrated significant and excellent correlations between the first and second measurements of all the indices ($0.98 < r < 0.99$, $p < 0.0001$). The limits of agreements for all indices between two investigators were determined as follows: BEANR; 0.00 ± 0.03 (mean $\pm$ 1.96 standard deviation), rSVD; 0.00 ± 0.02, SPECT; 0.00 ± 0.07.

The results of a comparison for CBF measurements by ^{123}I-IMP SPECT and each CTP method between the ischemic side and the healthy contralateral side are shown in Table 1. The CBF values of BEANR and ^{123}I-IMP SPECT were significantly different between the ischemic side and the healthy contralateral side ($p < 0.05$), but there were no significant differences in the CBF values of rSVD between the ischemic side and the healthy contralateral side ($p > 0.05$).

The correlation coefficients for the relationships between each CTP method and ^{123}I-IMP SPECT imaging are shown in Table 2 and Fig. 7. The CBF index of BEANR had a significant positive correlation with that of ^{123}I-IMP SPECT (healthy contralateral side: $r = 0.26$, $p < 0.01$; ischemic

Table 1 Comparison of CBF measurements by ^{123}I-IMP SPECT and each CTP method between the ischemic side and the healthy contralateral side

Methods		CBF values (ml/100 mg/min)		CBF index
		Healthy contralateral side	Ischemic side	
CTP	rSVD (mean ± SD)	35.7 ± 8.1	35.3 ± 8.6	0.99 ± 0.09
	BEANR (mean ± SD)	41.2 ± 8.5	37.6 ± 8.5*	0.92 ± 0.15
^{123}I-IMP SPECT (mean ± SD)		40.1 ± 11.9	33.0 ± 10.2*	0.83 ± 0.13

CTP CT perfusion, *rSVD* reformulated singular value decomposition, *BEANR* Bayesian estimation with advanced noise reduction, *SD* standard deviation

*Significant difference with healthy contralateral side for the same method ($p < 0.05$)

Table 2 Correlations of CBF values and index between CTP and SPECT

CBF		Healthy contralateral side		Ischemic side		CBF index	
		r	*P* value	*r*	*P* value	*r*	*P* value
CTP	rSVD	0.17	> 0.05	0.10	> 0.05	0.15	> 0.05
	BEANR	0.26	< 0.01	0.37	0.0001	0.55	< 0.0001

CTP CT perfusion, *rSVD* reformulated singular value decomposition, *BEANR* Bayesian estimation with advanced noise reduction

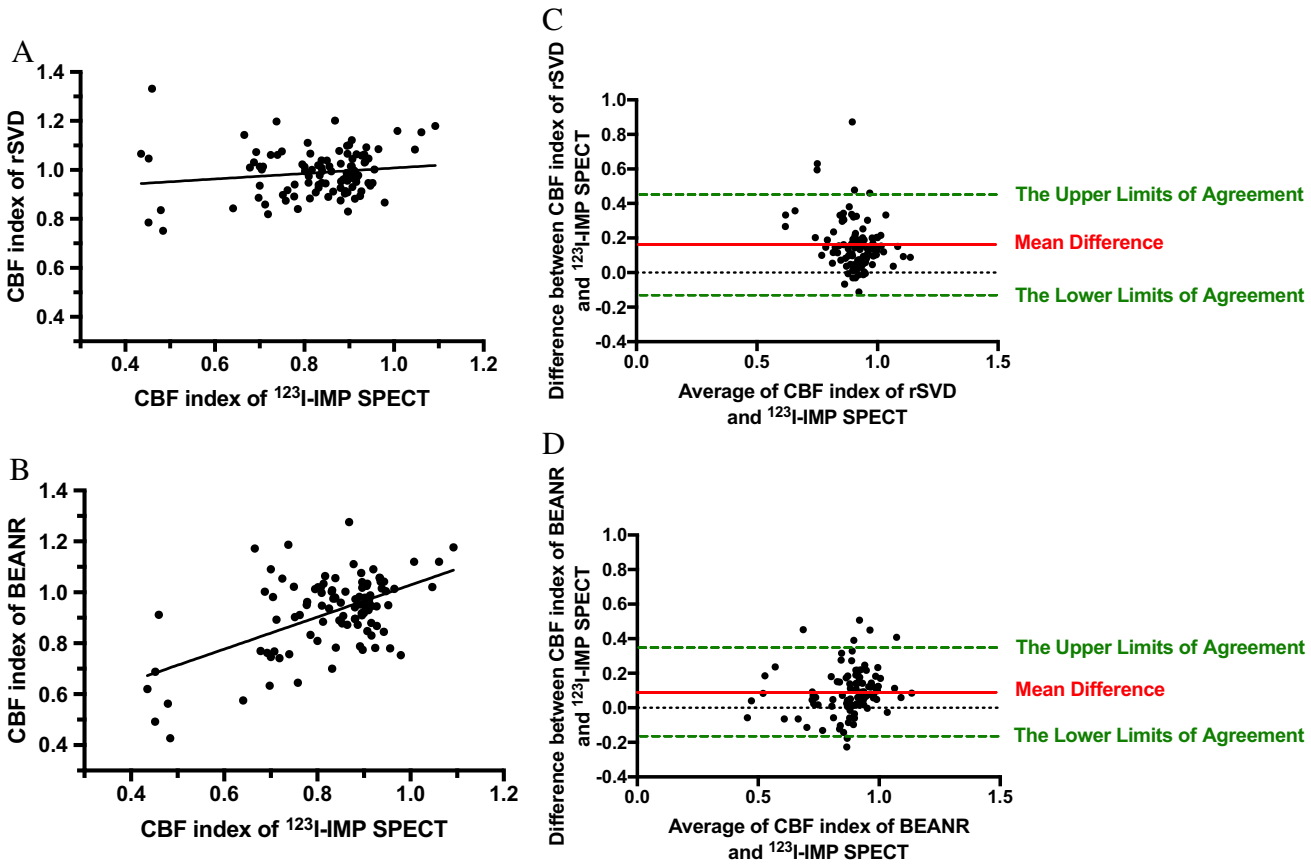

Fig. 7 Correlation and limits of agreement for the CBF index between ^{123}I-IMP SPECT and each CTP method. **A** ^{123}I-IMP SPECT correlates non-significantly with CTP-CBF using rSVD (CBF index: $r = 0.15$, $p > 0.05$). **B**.^{123}I-IMP SPECT correlates significantly with CTP-CBF using BEANR (CBF index: $r = 0.55$, $p < 0.0001$). **C** The limits of agreement for the CBF index of rSVD was determined as 0.16 ± 0.29. The mean difference for the CBF index of rSVD was assessed as 0.16 ± 0.01. **D** The limits of agreement for the CBF index of BEANR was determined as 0.09 ± 0.26. The mean difference for the BEANR CBF index of BEANR was assessed as 0.09 ± 0.01

side: $r = 0.37$, $p = 0.0001$; CBF index: $r = 0.55$, $p < 0.0001$), but there was no significant correlation between the rSVD method and ^{123}I-IMP SPECT (healthy contralateral side: $r = 0.17$, $p > 0.05$; ischemic side: $r = 0.10$, $p > 0.05$; CBF index: $r = 0.15$, $p > 0.05$). When comparing the mean difference in the CBF index assessed by each CTP method and ^{123}I-IMP SPECT, the BEANR method (mean ± standard error: 0.09 ± 0.01) differed significantly from the rSVD method (0.16 ± 0.01, $p < 0.001$). The limits of agreement for the CBF index between each CTP method and ^{123}I-IMP SPECT are shown in Fig. 7, showing that those of the BEANR method (−0.17 to 0.35) were smaller than those of the rSVD method (−0.13 to 0.45).

Discussion

Our results show not only that the CBF ratio calculated by BEANR correlated significantly better with SPECT than that calculated by rSVD but also that the mean difference in that ratio between BEANR and SPECT was significantly smaller than that between rSVD and SPECT (albeit with

similar limits of agreement). Furthermore, BEANR has greater potential to accurately assess the CBF ratio between ischemic and contralateral regions compared to the rSVD method in patients with CVD. We are aware of no other study that has compared the ability of BEANR directly with that of rSVD relative to an ^{123}I-IMP SPECT reference. Moreover, our two investigators produced significant and excellent interobserver agreement for each method with sufficiently small limits of agreement for clinical purposes, contrasting with previous research in which the reproducibility of measurements was assessed by Bland–Altman analysis to determine whether the mean difference and limits of agreements were small enough for clinical purposes [26–30]. Therefore, we consider our results reproducible both in academic studies and in routine clinical practice.

When comparing the CBF index between each CTP method and SPECT, the CBF index of the BEANR method showed a significantly good correlation with that of SPECT, whereas the CBF index of rSVD method did not show a significant correlation with that of SPECT in this study. In addition, the limits of agreements for all indices between two investigators were small enough for clinical purposes. Furthermore, the limits of agreement between BEANR and SPECT were small enough for clinical purposes and smaller than those for the rSVD method, with a significant difference in the mean difference between the BEANR and rSVD methods. These results may be expected given the following characteristics of the Bayesian estimation method for perfusion CT. First, it is a robust probabilistic method that minimizes the effects of oscillation, high noise levels, and tracer delay when estimating the residue function compared to other deconvolution methods [14, 15]. Second, phantom studies have shown that the Bayesian model offers more accurate estimates of perfusion values and reduced variability [31, 32]. Third, in a quantitative analysis study using a digital phantom, the estimation created strongly correlated perfusion maps with better agreement than those produced by a delay insensitive SVD algorithm [33]. Therefore, BEANR offers greater utility for the assessment of CBF than rSVD when evaluating cerebral ischemia in routine clinical practice, with the potential to complement SPECT. In addition, CTP for assessing CBF excluding high-blood-flow areas is well correlated with SPECT over the whole brain [5]. However, CTP including high-blood-flow areas was used to evaluate the correlation in this study. Therefore, the correlation between CTP and SPECT was poor as compared with the past literature [5]. In addition, despite the use of CTP in several recent clinical trials for subject selection, SVD methods are inherently vulnerable to noise errors because small changes in the magnitude of the time-density curve may cause large deviations in the residue function after deconvolution [34]. For these SVD problems, the ischemic core volumes derived by Bayesian estimation are less variable and more accurate [35], allowing BEANR to produce CBF maps that can more clearly identify the ischemic side.

There are several limitations to this study that may introduce bias. First, our small sample had various underlying clinical conditions, including acute and ischemic conditions. Second, the interval between CTP and SPECT was long enough in some patients that their conditions may have changed. Therefore, although we evaluated and compared different methods, we cannot claim to have compared brain perfusion by CTP and SPECT under the same conditions. Third, we only tested CBF maps of CTP because these could be compared directly with SPECT. Although CBF maps are the optimal CTP parameter for assessing infarct cores in which relative CBF is < 30% in normal tissue [36], other CTP parameters, such as cerebral blood volume, MTT, time to peak, and T_{max}, should be evaluated in patients with CVD to improve measurement compared to the rSVD method. Fourth, we could not individually assess the effect of the Bayesian estimation method and four-dimensional similarity filter on CBF measurements as both techniques are combined in the software package used. Instead, we compared two commercially available techniques to assess which CBF measurements corresponds best with ^{123}I-IMP SPECT when used in clinical practice. Fifth, this study did not evaluate the diagnostic accuracy of CBF measurement by CTP using BEANR and rSVD. We will therefore evaluate the diagnostic accuracy of CBF measurement by CTP and compare ischemia detection capabilities of two CTP methods in future studies.

In conclusion, the newly commercially available BEANR method has a better potential for measuring CBF in CTP than the rSVD method compared to ^{123}I-IMP SPECT in patients with CVD. The BEANR method appears to be more suitable than the rSVD method for calculating CBF in patients with CVD.

Author contribution All authors contributed to the study conception and design. Material preparation and data collection were performed by Ichiro Nakahara, and analysis was performed by Satomu Hanamatsu. The first draft of the manuscript was written by Kazuhiro Murayama, and all authors commented on previous versions of the manuscript. All authors read and approved the final manuscript.

Funding This work was supported by Canon Medical Systems Corporation.

Data availability Data generated or analyzed during the study are available from the corresponding author by request.

Code availability Software application: Vitrea workstation (Brain Perfusion 4D, Vital Images, Minnetonka, MN, USA).

Declarations

Ethics approval This retrospective study was approved by the Institutional Review Board of Fujita Health University (Toyoake, Japan).

Consent to participate Written informed consents were waived for all subjects in this retrospective study according to the approval of the local ethics committee (Fujita Health University, Toyoake, Japan).

Consent for publication Written informed consents were waived for all subjects in this retrospective study according to the approval of the local ethics committee (Fujita Health University, Toyoake, Japan).

Conflict of interest Kazuhiro Murayama, Kazuhiro Katada, Yoshiharu Ohno, and Hiroshi Toyama have received a research grant from Canon Medical Systems Corporation, which also supported this work technically. Ewoud J. Smit has received speaker honorarium from Canon Medical Systems Corporation. Mathias Prokop has received personal fees from Bracco, Bayer, Canon Medical Systems, and Siemens Healthineers and grants from Canon Medical Systems and Siemens Healthineers. Kazuhiro Katada is consultant to Canon Medical Systems Corporation. Yoshihiro Ikeda and Kenji Fujii are employees of Canon Medical Systems. The other authors declare that they have no conflict of interest.

References

1. Klotz E, König M (1999) Perfusion measurements of the brain: using dynamic CT for the quantitative assessment of cerebral ischemia in acute stroke. Eur J Radiol 30:170–184. https://doi.org/10.1016/s0720-048x(99)00009-1
2. Mayer TE, Hamann GF, Baranczyk J et al (2000) Dynamic CT perfusion imaging of acute stroke. AJNR Am J Neuroradiol 21:1441–1449
3. Lev MH, Segal AZ, Farkas J et al (2001) Utility of perfusion-weighted CT imaging in acute middle cerebral artery stroke treated with intra-arterial thrombolysis: prediction of final infarct volume and clinical outcome. Stroke 32:2021–2028. https://doi.org/10.1161/hs0901.095680
4. Sakai F, Nakazawa K, Tazaki Y et al (1985) Regional cerebral blood volume and hematocrit measured in normal human volunteers by single-photon emission computed tomography. J Cereb Blood Flow Metab 5:207–213. https://doi.org/10.1038/jcbfm.1985.27
5. Murayama K, Toyama H, Hayakawa M et al (2014) Voxel-based correlation between whole-brain CT perfusion with 320-row area detector CT and iodine 123 iodoamphetamine brain perfusion spect in patients with cerebrovascular disease. J Comput Assist Tomogr 38:639–646. https://doi.org/10.1097/rct.0000000000000110
6. Siebert E, Bohner G, Dewey M et al (2009) 320-slice CT neuroimaging: initial clinical experience and image quality evaluation. Br J Radiol 82:561–570. https://doi.org/10.1259/bjr/27721218
7. Berkhemer OA, Fransen PS, Beumer D et al (2015) A randomized trial of intraarterial treatment for acute ischemic stroke. N Engl J Med 372:11–20. https://doi.org/10.1056/NEJMoa1411587
8. Campbell BC, Mitchell PJ, Kleinig TJ et al (2015) Endovascular therapy for ischemic stroke with perfusion-imaging selection. N Engl J Med 372:1009–1018. https://doi.org/10.1056/NEJMoa1414792
9. Goyal M, Demchuk AM, Menon BK et al (2015) Randomized assessment of rapid endovascular treatment of ischemic stroke. N Engl J Med 372:1019–1030. https://doi.org/10.1056/NEJMoa1414905
10. Wu O, Østergaard L, Weisskoff RM, Benner T, Rosen BR, Sorensen AG (2003) Tracer arrival timing-insensitive technique for estimating flow in MR perfusion-weighted imaging using singular value decomposition with a block-circulant deconvolution matrix. Magn Reson Med 50:164–174. https://doi.org/10.1002/mrm.10522
11. Fieselmann A, Kowarschik M, Ganguly A, Hornegger J, Fahrig R (2011) Deconvolution-based CT and MR brain perfusion measurement: theoretical model revisited and practical implementation details. Int J Biomed Imaging 2011:467563. https://doi.org/10.1155/2011/467563
12. Konstas AA, Goldmakher GV, Lee TY, Lev MH (2009) Theoretic basis and technical implementations of CT perfusion in acute ischemic stroke, part 2: technical implementations. AJNR Am J Neuroradiol 30:885–892. https://doi.org/10.3174/ajnr.A1492
13. Murayama K, Katada K, Hayakawa M, Toyama H (2017) Shortened mean transit time in CT perfusion with singular value decomposition analysis in acute cerebral infarction: quantitative evaluation and comparison with various CT perfusion parameters. J Comput Assist Tomogr 41:173–180. https://doi.org/10.1097/rct.0000000000000498
14. Mouridsen K, Friston K, Hjort N, Gyldensted L, Ostergaard L, Kiebel S (2006) Bayesian estimation of cerebral perfusion using a physiological model of microvasculature. Neuroimage 33:570–579. https://doi.org/10.1016/j.neuroimage.2006.06.015
15. Boutelier T, Kudo K, Pautot F, Sasaki M (2012) Bayesian hemodynamic parameter estimation by bolus tracking perfusion weighted imaging. IEEE Trans Med Imaging 31:1381–1395. https://doi.org/10.1109/tmi.2012.2189890
16. Nael K, Mossadeghi B, Boutelier T et al (2015) Bayesian estimation of cerebral perfusion using reduced-contrast-dose dynamic susceptibility contrast perfusion at 3T. AJNR Am J Neuroradiol 36:710–718. https://doi.org/10.3174/ajnr.A4184
17. Nael K, Tadayon E, Wheelwright D et al (2019) Defining ischemic core in acute ischemic stroke using CT perfusion: a multiparametric bayesian-based model. AJNR Am J Neuroradiol 40:1491–1497. https://doi.org/10.3174/ajnr.A6170
18. Smith MR, Lu H, Trochet S (2004) R Frayne (2004) Removing the effect of SVD algorithmic artifacts present in quantitative MR perfusion studies. Magn Reson Med. 51(3):631–4. https://doi.org/10.1002/mrm.20006
19. Murayama K, Katada K, Nakane M et al (2009) Whole-brain perfusion CT performed with a prototype 256-detector-row CT system: initial experience. Radiology 250:202–211. https://doi.org/10.1148/radiol.2501071809
20. Ichihara T, Ogawa K, Motomura N, Kubo A, Hashimoto S (1993) Compton scatter compensation using the triple-energy window method for single- and dual-isotope SPECT. J Nucl Med 34:2216–2221
21. Ishii K, Hanaoka K, Okada M et al (2012) Impact of CT attenuation correction by SPECT/CT in brain perfusion images. Ann Nucl Med 26:241–247. https://doi.org/10.1007/s12149-011-0567-y
22. Inui Y, Ichihara T, Uno M et al (2018) CT-based attenuation correction and resolution compensation for I-123 IMP brain SPECT normal database: a multicenter phantom study. Ann Nucl Med 32:311–318. https://doi.org/10.1007/s12149-018-1248-x
23. Kudo K, Terae S, Katoh C et al (2003) Quantitative cerebral blood flow measurement with dynamic perfusion CT using the vascular-pixel elimination method: comparison with H2(15)O positron emission tomography. AJNR Am J Neuroradiol 24:419–426
24. Kouchi T, Tanabe Y, Smit EJ et al (2020) Clinical application of four-dimensional noise reduction filtering with a similarity algorithm in dynamic myocardial computed tomography perfusion

imaging. Int J Cardiovasc Imaging 36:1781–1789. https://doi.org/10.1007/s10554-020-01878-6
25. Tsuneta S, Oyama-Manabe N, Kameda H et al (2020) Improvement of image quality on low-dose dynamic myocardial perfusion computed tomography with a novel 4-dimensional similarity filter. Medicine (Baltimore) 99:e20804. https://doi.org/10.1097/MD.0000000000020804
26. Bland JM, Altman DG (1986) Statistical methods for assessing agreement between two methods of clinical measurement. Lancet 1:307–310
27. Ohno Y, Yui M, Yoshikawa T et al (2021) 3D Oxygen-Enhanced MRI at 3T MR System: comparison with thin-section CT of quantitative capability for pulmonary functional loss assessment and clinical stage classification of COPD in Smokers. J Magn Reson Imaging 53:1042–1051. https://doi.org/10.1002/jmri.27441
28. Ohno Y, Yui M, Chen Y, Kishida Y, Seki S, Yoshikawa T (2019) Gadolinium-based blood volume mapping from MRI With ultrashort TE versus CT and SPECT for predicting postoperative lung function in patients with non-small cell lung cancer. AJR Am J Roentgenol 212:57–66. https://doi.org/10.2214/ajr.18.20095
29. Ohno Y, Koyama H, Matsumoto K et al (2011) Differentiation of malignant and benign pulmonary nodules with quantitative first-pass 320-detector-row perfusion CT versus FDG PET/CT. Radiology 258:599–609. https://doi.org/10.1148/radiol.10100245
30. Ohno Y, Nishio M, Koyama H et al (2013) Comparison of quantitatively analyzed dynamic area-detector CT using various mathematic methods with FDG PET/CT in management of solitary pulmonary nodules. AJR Am J Roentgenol 200:W593-602. https://doi.org/10.2214/ajr.12.9197
31. Sasaki M, Kudo K, Ogasawara K, Fujiwara S (2009) Tracer delay-insensitive algorithm can improve reliability of CT perfusion imaging for cerebrovascular steno-occlusive disease: comparison with quantitative single-photon emission CT. AJNR Am J Neuroradiol 30:188–193. https://doi.org/10.3174/ajnr.A1274
32. Kudo K, Boutelier T, Pautot F et al (2014) Bayesian analysis of perfusion-weighted imaging to predict infarct volume: comparison with singular value decomposition. Magn Reson Med Sci 13:45–50
33. Sasaki M, Kudo K, Boutelier T et al (2013) Assessment of the accuracy of a Bayesian estimation algorithm for perfusion CT by using a digital phantom. Neuroradiology 55:1197–1203. https://doi.org/10.1007/s00234-013-1237-7
34. Ostergaard L, Weisskoff RM, Chesler DA, Gyldensted C, Rosen BR (1996) High resolution measurement of cerebral blood flow using intravascular tracer bolus passages. Part I: Mathematical approach and statistical analysis. Magn Reson Med 36:715–725. https://doi.org/10.1002/mrm.1910360510
35. Sakai Y, Delman BN, Fifi JT et al (2018) Estimation of ischemic core volume using computed tomographic perfusion. Stroke 49:2345–2352. https://doi.org/10.1161/STROKEAHA.118.021952
36. Campbell BC, Christensen S, Levi CR et al (2011) Cerebral blood flow is the optimal CT perfusion parameter for assessing infarct core. Stroke 42:3435–3440. https://doi.org/10.1161/STROKEAHA.111.618355